PHYSICAL REVIEW B

SOLID STATE

THIRD SERIES, VOL. 7, NO. 9 1 MAY 1973

Axial- to Planar-Channeling Transition*

G. Della Mea, A. V. Drigo, S. Lo Russo, and P. Mazzoldi
Istituto di Fisica dell'Università, Unità del Gruppo Nazionale di Struttura della Materia del Consiglio Nazionale delle Ricerche, Padova, Italy

G. G. Bentini, A. Desalvo,† and R. Rosa
Laboratorio di Chimica e Tecnologia dei Materiali e Componenti per l'Elettronica, Consiglio Nazionale delle Ricerche, Bologna, Italy
(Received 31 July 1972)

Axial and planar channeling of 1.0- to 2.8-MeV protons in silicon was studied both by transmission in some μm-thick crystals and by Rutherford backscattering. Transmission experiments were simulated by a Monte Carlo program. A sharp transition between axial and planar channeling is observed by measuring both the effective stopping number B of channeled particles and the dechanneled fraction. Computer simulations exhibit the same features and show that at the transition, the transverse energy component is such as to produce a maximum probability of hitting the atoms. These experiments also give some criteria for the interpretation of backscattering measurements.

I. INTRODUCTION

Various authors have argued about the "logical" priority either of axial or planar channeling.[1,2] On the other hand, some experiments and calculations show a sharp separation between axial- and planar-channeling effects.[3–6] In particular Dearnaley *et al.*[7] examined in detail the relationship between axial and planar channeling, studying the inclined axial patterns of protons in thin crystals of silicon. A model has been developed which shows qualitatively how axial channeling may be regarded as distinct from planar channeling; the two kinds of channeling being separated by a saddle-shaped potential barrier.[7]

The present study was undertaken in order to clarify the relationship between axial and planar channeling by observing new parameters.

The energy loss of protons transmitted through thin single crystals of silicon was studied with the proton beam incident at a small angle θ to a low-index direction but still lying within one of the low-index planes of the crystal. Moreover the wide-angle Rutherford scattering was analyzed as a function of θ, in order to obtain the dependence of the dechanneled-beam fraction χ on the misalignment angle.

The experimental results are compared with the theoretical expectations obtained with a Monte Carlo program.

II. EXPERIMENTAL PROCEDURE

A detailed account of the experimental technique has been reported elsewhere.[8] Only a short description will be presented here.

The silicon crystals for the energy-loss measurements were thinned according to Meek's technique,[9] the target thickness ranging from 1.5 to 6.0 μm. The thickness was checked by measuring the energy loss of transmitted particles in a random orientation, using the tabulated stopping power of Williamson *et al.*[10]

The crystals were mounted on a three-axes goniometer, and the energy of the transmitted beam was analyzed by means of a large silicon-surface-barrier detector placed just behind the sample. The acceptance angle of the detector was about 100°.

The incident beam from the 5.5-MeV Van de Graaff accelerator of Laboratori Nazionali di Legnaro was collimated to better than 0.05°. The beam current was kept to the order of 10^{-10} A.

The energy distribution of the backscattered particles was measured by means of a silicon-surface-barrier detector at about 160° to the incident beam. The beam current was of the order of 10^{-9} A to

avoid too high counting rates and the distortion in pulse-amplitude spectra associated with pulse pile up.

III. COMPUTER MODEL

The computer model is an extension of a previous one devised for the study of the penetration of heavy ions of some tens of keV and is described in detail elsewhere.[11] Therefore, in the following we outline only the main modifications introduced for the present calculations.

The most important one concerns the impact-parameter dependence of the energy loss. We use the following expression due to Lindhard[1] and employed for calculations by other authors[12]:

$$-\frac{dE}{dx}=\left(-\frac{dE}{dx}\right)_R\left(\alpha+\frac{(1-\alpha)\rho(b)}{NZ_2}\right) , \tag{1}$$

where N and Z_2 have the usual meaning and the index R refers to the stopping power in the random case. We use α in place of $1-\alpha$ in the original formula in order to maintain the same notation of our previous experimental works.[8]

The electron density was obtained from the usual expression

$$\rho(b)=\frac{A}{d}\int_{-d/2}^{d/2}\rho_{at}(b^2+z^2)^{1/2}\,dz , \tag{2}$$

with ρ_{at} given by

$$\rho_{at}(r)=\frac{3Z_2}{4\pi}\,\frac{C_1^2a^2}{(r^2+C_1^2a^2)^{5/2}} \tag{2'}$$

[see Eq. (2.6′) of Ref. 1 for the meaning of symbols]. A is a normalization constant, whose value is not very different from one, chosen in such a way that the total number of electrons is Z_2 in a cylinder of height d and volume N^{-1}.

We chose $\alpha=0.5$, which is the value that best fits the experimental results for best channeled particles in the most open channels in Si in our energy range.[8] Of course α can be considered as an adjustable parameter to improve the fit to the experimental results: In any case it must be remembered that α varies with energy.[8,13] In other words the use of Eq. (1) does not imply for us any assumption on the validity of equipartition rule.

To evaluate the random stopping power we preferred to use, in place of the values tabulated by Williamson *et al.*,[10] the simpler analytical expression due to Lindhard and Scharff[14] which gives the same results in our energy range:

$$-\left(\frac{dE}{dx}\right)_R=\frac{4\pi Z_1^2e^4}{mv^2}\,NZ_2L , \tag{3}$$

where the symbols have the usual meaning and

$$L=1.36\frac{v}{v_0Z_2}-0.016\left(\frac{v}{v_0Z_2}\right)^3 \tag{3'}$$

($v_0=e^2/\hbar$ is the Bohr velocity).

The choice of Eq. (1) requires some comments. First of all we computed transmitted energy spectra assuming an impact-parameter dependence as given by Appleton *et al.*[2] and used in our previous papers.[8] According to this procedure the contribution to the stopping power is split in two parts: one due to valence electrons, independent of position, and the other one due to core electrons. The contribution of the latter ones is assumed to be zero for impact parameters greater than the adiabatic limit $b_{max}=\hbar v/\Delta E$, where ΔE is the binding energy of the electron shell. For lower impact parameters b the core contribution to the energy loss scales in the ratio $\ln(b_{max}/b)/\ln(2mv^2/\Delta E)$. Figure 1 compares the impact parameter dependence in the two cases. As it is clearly seen this model gives too mild a dependence on the impact parameter, and the computed energy spectra are not all comparable with the experimental ones. In particular this model gives a value much lower than the random stopping power when averaged over all impact parameters, because the spatial region in which the stopping power is larger than the random one is too small. We notice that the use of Eq. (1) allows us to understand the discrepancy between the results for ⟨110⟩ and ⟨111⟩ axes which remained unexplained in our previous work.[8] In fact from Fig. 4 of the second paper of Ref. 8 we obtain a ratio between the stopping powers along ⟨111⟩ and ⟨110⟩ axes equal to 1.2, which is the value given by Eq. (1), using the two channel radii, respectively.

Using the proper modification of Eq. (1) for the

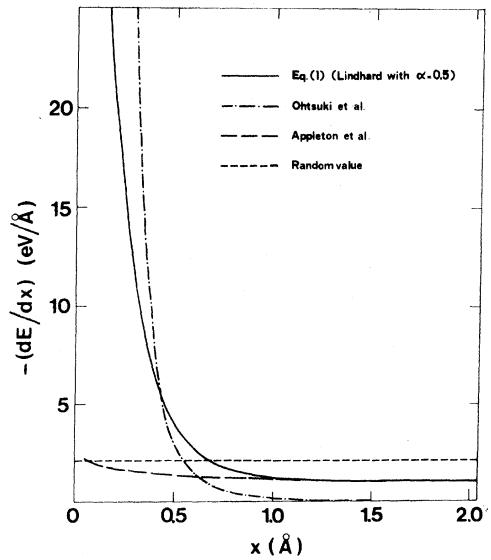

FIG. 1. The local stopping power as a function of the distance from the atomic row for 2.8-MeV protons in the ⟨110⟩ channel of silicon.

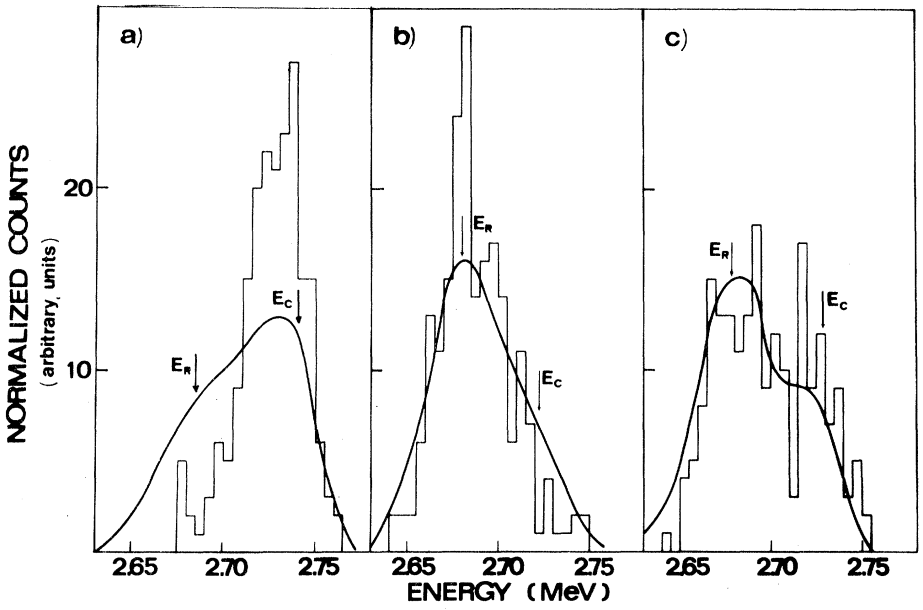

FIG. 2. Experimental (continuous curve) and computed (hystograms) energy spectra of 2.8-MeV protons transmitted through a 5.6-μm-thick Si crystal. E_C and E_R are the energies of the Gaussian peak fitted to the high-energy side of the spectrum and the energy of the random peak (not shown in figure). The tilting is along the $\{110\}$ plane and the angular distance from the $\langle 110 \rangle$ axis is (a) 0°, (b) 0.4°, (c) 0.8°.

planar case and a slightly higher value of α (0.60–0.65), appropriate for lower energies, we obtain an impact parameter dependence not very different from the one obtained phenomenologically by Robinson for 0.4-MeV protons channeled along the $\{110\}$ and $\{111\}$ planes in Si[15]: The maximum discrepancies amount to 15 and 30%, respectively.

As a consequence the use of Eq. (1), even though it lacks of sound theoretical foundations, seems to be a reasonable approach from a semiempirical point of view.

No computation was on the contrary made using the more recent theoretical expression found by Ohtsuki *et al.*[16] In fact in its more tractable analytical form (i.e., the classical one using Lindhard's electron density) it gives too low values at the midchannel axis (cf. Fig. 1 of this paper and Fig. 3 of Ohtsuki *et al.*, Ref. 16).

Another modification of our previous program concerns the angle for electron multiple scattering which was replaced by the more common expression valid in the high-velocity limit[17]:

$$\langle \theta_{el}^2 \rangle^{1/2} = \left(\frac{m}{2M_1} \frac{\Delta E}{E} \right)^{1/2} . \tag{4}$$

No allowance was made for a thin-surface oxide layer, although according to recent calculations it seems to be important.[18] On the contrary the divergence of the incident beam was taken into account: The incidence angle was varied by a certain amount picked at random and weighted, as usual, over a triangular distribution equivalent to a Gaussian of full width at half-maximum (FWHM) equal to the experimental beam divergence (0.05°).

Finally we simulated the finite-energy resolution of our detecting equipment (29-keV FWHM) by using a procedure similar to the one outlined above.

IV. RESULTS

A. Transmission Measurements

Figure 2(a) shows the energy spectrum of 2.8-MeV protons transmitted parallel to the $\langle 110 \rangle$ axis of a Si crystal 5.6 μm thick. The most probable energy loss of the channeled particles was taken as the peak of a Gaussian curve fitted to the high-energy side of the spectrum.[2,8] E_C is the energy of the channeled Gaussian peak and E_R the energy of the random peak obtained when the beam is incident in a random orientation. Figures 2(b) and 2(c) show the energy spectrum of protons emergent from the same crystal when the beam is misaligned from the $\langle 110 \rangle$ axis, but within the $\{110\}$ plane. The misalignment angle is (b) 0.4° and (c) 0.8°. The histograms show the results of our Monte Carlo program simulating the same experimental conditions.

Figure 3 shows the transmission energy spectra of 1-MeV protons incident on a Si crystal 2.45 μm thick. The histograms give the results of the Monte Carlo calculations. The beam misalignment angles from the $\langle 110 \rangle$ axis, within the $\{110\}$ plane, are (a) 0°, (b) 0.8°, and (c) 1.6°.

Figure 4 shows the transmitted energy spectra of 2.0-MeV protons transmitted through a 6.2-μm silicon crystal. We note that the scanning is through $\langle 110 \rangle$ axis within $\{111\}$ plane. The beam misalignment angles are (a) 0°, (b) 0.2°, and (c) 0.6°.

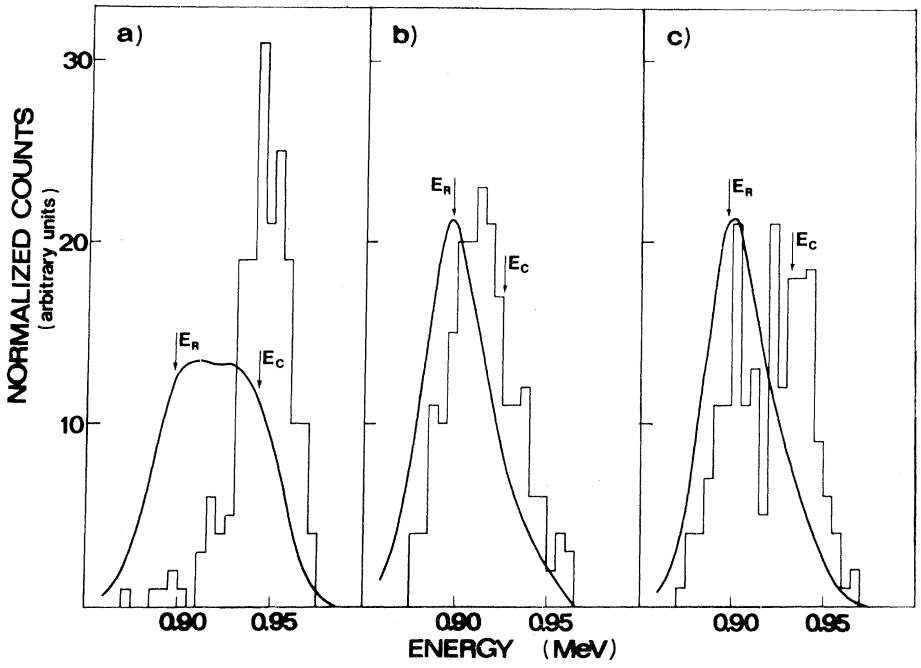

FIG. 3. Experimental and computed energy spectra of 1.0-MeV protons transmitted through a 2.45-μm-thick Si crystal. The meaning of symbols is the same as in Fig. 2. The tilting is along the {110} plane and the angular distance from the ⟨110⟩ axis is (a) 0°, (b) 0.8°, (c) 1.5°.

In all these figures the angles correspond to (a) axial channeling, (b) a "transition condition" (maximum value of effective stopping number $\bar{B}$, to be defined below) and (c) planar channeling.

The agreement between computed and experimental energy spectra is not very satisfactory, especially at low energies. However, both show the same general variation of the shape of the spectrum with tilt angle and position of the channeled peak. About the latter point we must point out that we did not try a Gaussian fit for the channeled particles in the computed spectra because of the low statistics (only 200 total incident particles, in order not to make the computing time prohibitively large). The major disagreement lies in the fact that computations underestimate dechanneling, in particular at 0° incidence. This can be due to the following reasons.

(i) The experimental incident beam may have a "tail" of particles scattered by the slit system with a lower energy and a higher angular divergence. Of course no simulation was tried for this component.

(ii) The impact-parameter-dependent stopping function may be steeper, so that intermediate paths should correspond to higher energy losses.

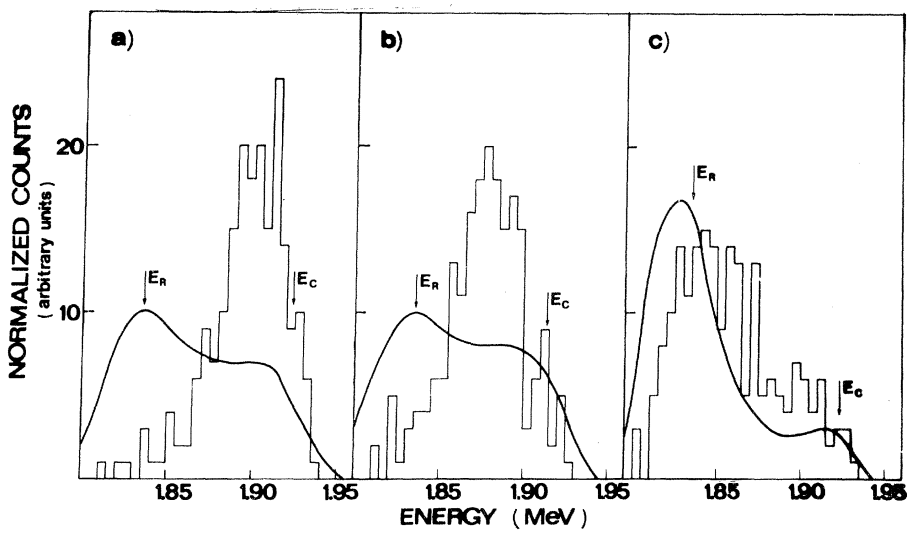

FIG. 4. Experimental and computed energy spectra for 2.0-MeV protons transmitted through a 6.2-μm-thick Si crystal. The meaning of symbols is the same as in Fig. 2. The tilting is along the {111} plane and the angular distance from the ⟨110⟩ axis is (a) 0°, (b) 0.2°, (c) 0.6°.

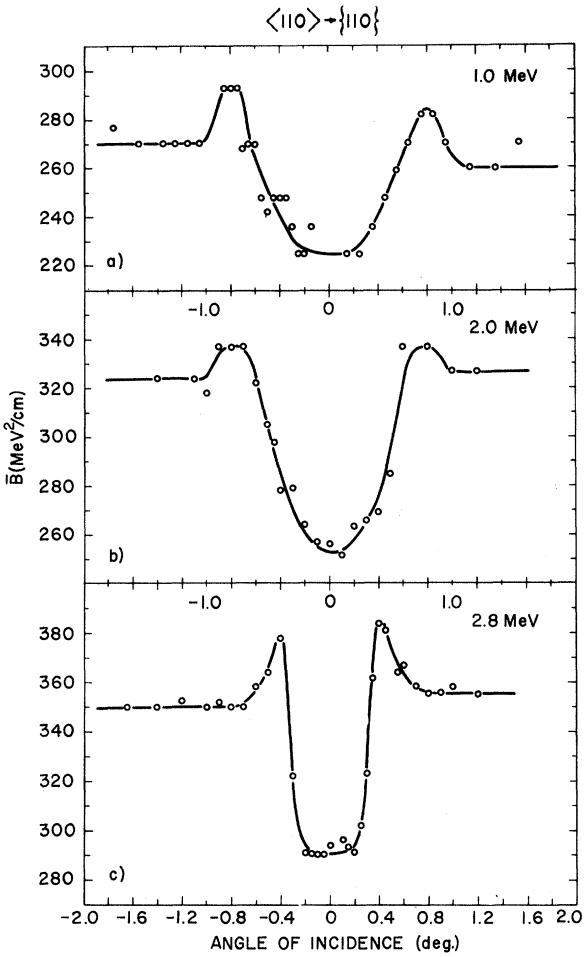

FIG. 5. Effective stopping number $\bar{B}(\bar{E})$ vs tilt angle from the ⟨110⟩ axis within the {110} plane. The energy (in MeV) of the incident beam is (a) 1.0, (b) 2.0, (c) 2.8; the crystal thickness (in μm) is (a) 2.45, (b) 6.1, (c) 5.6; the random $\bar{B}$ values are 410, 528, and 586 MeV^2/cm, respectively. The estimated error amounts to $\sim \pm 2\%$.

It must be noticed that for a completely random incidence we obtain a spectrum in excellent agreement with experiments.

(iii) It may be that there is more multiple scattering than we simulated with our mechanisms, as has been noticed recently also by other authors.[19] In particular we recall that we neglected surface oxide scattering.

In any case the quantitative inaccuracy on the dechanneled side of the spectrum does not impair the results on the channeled side. The general agreement shown in the main features gives confidence in extracting all the available informations from the experiments.

We analyze the energy-loss data in terms of the experimental effective stopping number $\bar{B}$. The effective stopping number is defined as $B(E)/E = -dE/dx$. The experimental value $\bar{B}$ is calculated by the formula[20]

$$\bar{B}(\bar{E}) = \frac{1}{\Delta x}\int_{E_f}^{E_i} E\,dE = \frac{E_i^2 - E_f^2}{2\Delta x}\ , \qquad (5)$$

where E_i is the energy of the incident ion, E_f is the energy of the emergent ion (which in the case of channeled ions correspond to our E_C of Figs. 2–4), and Δx the crystal thickness. We point out that $\bar{B}(\bar{E})$ is almost independent of crystal thickness.[8,20]

Figure 5 shows the effective stopping number $\bar{B}(\bar{E})$ as a function of the beam misalignment from the ⟨110⟩ axis, but within the {110} plane. The energy of the incident beam is (a) 1.0 MeV, (b) 2.0 MeV, and (c) 2.8 MeV. It appears that in the transition from axial to planar channeling the stopping number has a maximum above the planar value, but always lower than the random one. We notice that a similar trend can be obtained by connecting the peaks of the energy loss distribution shown very recently in Fig. 1 of second paper in Ref. 19 for 21.6-MeV I ions in Ag, even though the experimental technique is somewhat different.

The same behavior is shown in Figs. 6 and 7 for the transition from an axis to the most open plane intersecting it (see figure captions for proton energy and crystal orientation). It must be remarked that in these cases the $\bar{B}$ values for axis and plane are the same.[2,8]

As is well known information on dechanneling can be obtained from transmitted energy spectra.[21,22] The spectra were analyzed as follows: (a) channeled spectrum, i.e., the area under the high-energy Gaussian peak described above; (b) random spectrum, obtained by normalizing the peak value of a spectrum observed in a random orientation at the value of the aligned spectrum at energy E_R; (c) intermediate spectrum, which includes the particles with energy between E_C and E_R remaining after subtracting (a) and (b)—these particles correspond both to particles dechanneled at various depth and to relatively low-impact-parameter channeled paths; (d) high-energy-loss spectrum, i.e., what remains at energies lower than E_R after subtracting (b)—this component is appreciable only for off-axis orientation and is of the order of 5%.

This analysis is of course less detailed than the one of Ref. 22. On the other hand it differs from the one of Ref. 21 because we do not analyze region (c) directly.

Figure 8 gives the channeled and random fractions for 2.8-MeV protons versus incidence angle. It shows clearly that in the axial-to-planar transition region the dechanneling is the highest.

This trend is depicted also by our computer simulations shown in Table I. Some words must be

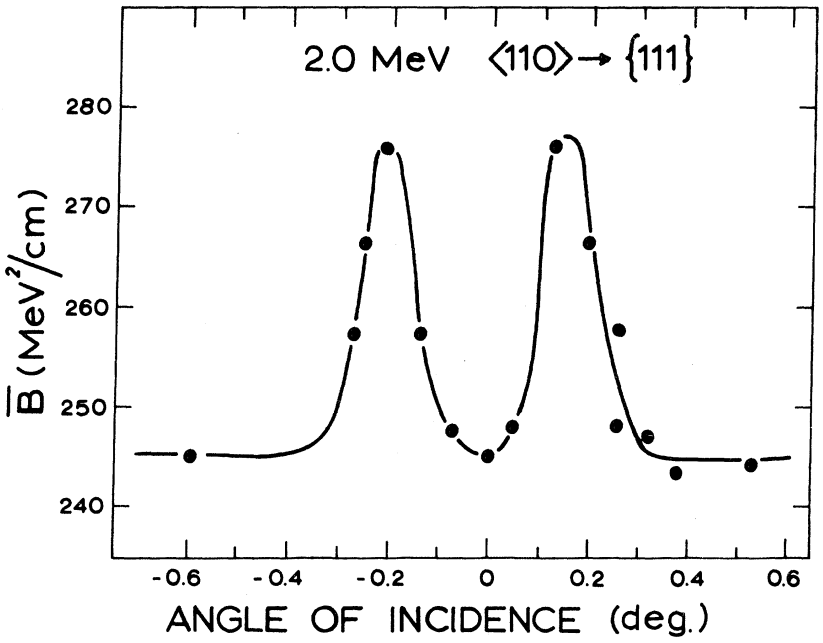

FIG. 6. Effective stopping number $\bar{B}(\bar{E})$ as a function of tilt angle from the ⟨110⟩ axis within the most open intersecting plane {111}. The energy of the incident beam is 2.0 MeV, the crystal thickness 6.2 μm, and the random $\bar{B}$ value 528 MeV^2/cm.

spent to describe the criteria used to define the channeled fraction $1-\chi$ in these simulations.

First of all, in order to compare with the experimentally defined channeled spectrum (a), we also included in the channeled component ions which covered more than 90% of the thickness along a channeled path. In fact the energy of these ions coincides, within the energy resolution, with that of the ions channeled along the whole thickness. However, this part amounts at most to ~8% of the total channeled particles.

Another problem arose in the case of axial channeling, owing to the wandering of ions. One possible criterion to define dechanneling in this case could be the introduction of a critical approach distance to the atomic row. However, the appropriate value for this distance is somewhat arbitrary[5] and our results turned out to be sensitive to the choice made. Therefore we used a statistical criterion, by which we compare the fraction of encounters below a certain impact parameter {taken equal to a_{TF} [where a_{TF} is the Thomas–Fermi screening length, equal to $a_{TF}=a_0 \cdot 08853\ (Z_1^{2/3}+Z_2^{2/3})^{-1/2}$]} with the random value given by the ratio of

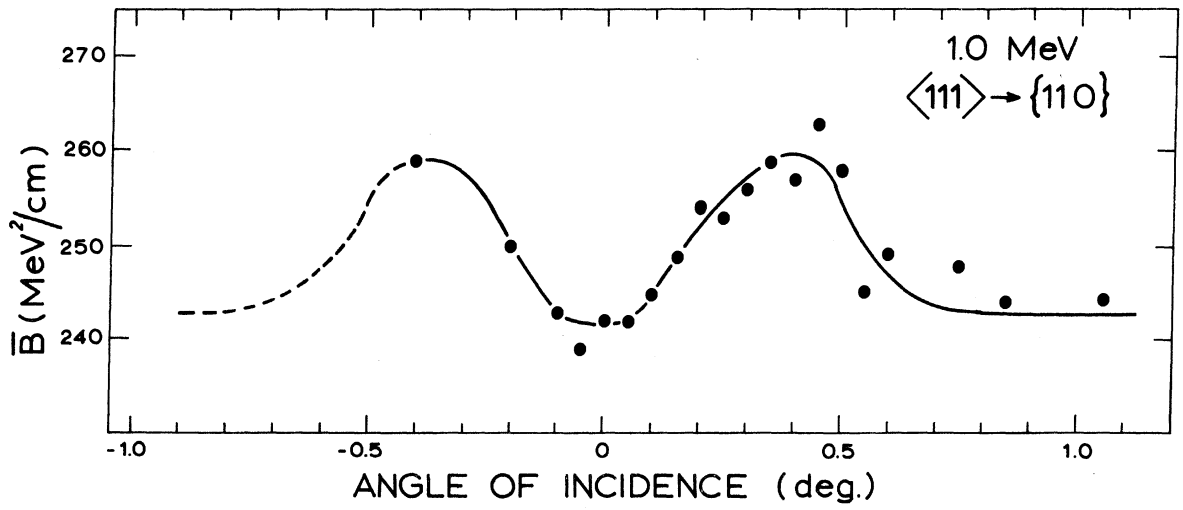

FIG. 7. Effective stopping number $\bar{B}(\bar{E})$ as a function of tilt angle from the ⟨111⟩ axis within the {110} plane. The energy of the incident beam is 1.0 MeV, the crystal thickness 5.25 μm, and the random $\bar{B}$ value 410 MeV^2/cm.

TABLE I. Computed values of the channeled fraction $1-\chi$ for various axial-planar transitions. θ is the tilt angle.

⟨110⟩→{110}	θ	0°	0.8°	1.5°	2.9°
1.0 MeV 2.45 μm	$1-\chi$	91%	16%	40%	53%
⟨110⟩→{110}	θ	0°	0.4°	0.8°	1.65°
2.8 MeV 5.6 μm	$1-\chi$	92%	2%	33%	46%
⟨110⟩→{111}	θ	0°	0.2°	0.6°	•••
2.0 MeV 6.2 μm	$1-\chi$	82%	2%	15%	•••

the areas $\pi a_{TF}^2/\pi r_{ch}^2$ (where r_{ch}, the channel radius, is given by $\pi r_{ch}^2 = (Nd)^{-1}$, in Lindhard's notation.[1]) This comparison is made at each axial channel change. This statistical criterion turns out to be satisfied also when the ion leaves a planar channel; insuring therefore the self-consistency of the data shown in Table I.

By comparing with experimental results, we see that the qualitative trend is reproduced; in particular, dechanneling is the highest in the transition region. However, dechanneling is greater underestimated in the axial case, as already mentioned in the analysis of transmitted energy spectra, and is overestimated in the transition region. It must be pointed out that in the latter region the analysis of experimental data is more liable to errors, owing to the strong overlapping of the different parts of the energy spectrum. In any case Monte Carlo simulations rather emphasize the transition region compared to experiments, ensuring that such a transition exists quite independently on the particular dechanneling mechanisms taken into account.

B. Backscattering Measurements

The increase in the dechanneled fraction in the transition region has been checked measuring the yield of 1.0-MeV protons backscattered as a function of tilt angle for the transition ⟨110⟩→{110}.

The dechanneled fraction χ as a function of the depth was calculated from the backscattered spectra following the procedure described in the Appendix and using the value of the energy loss obtained from the transmission measurements for each tilt angle.

In Fig. 9 we report the dechanneled fraction χ versus the angle of incidence to ⟨110⟩ direction within {110} plane at the depths of 0.5, 2.5, and 4.5 μm. Here again we observe that the transition from axial to planar channeling is marked by an increase in dechanneled fraction as expected. This increase is similar to the well known "shoulders" in the channeling to random transition. However it is important to point out that the maximum scattering yield is always lower than the random one.

As the beam becomes more and more dechan-

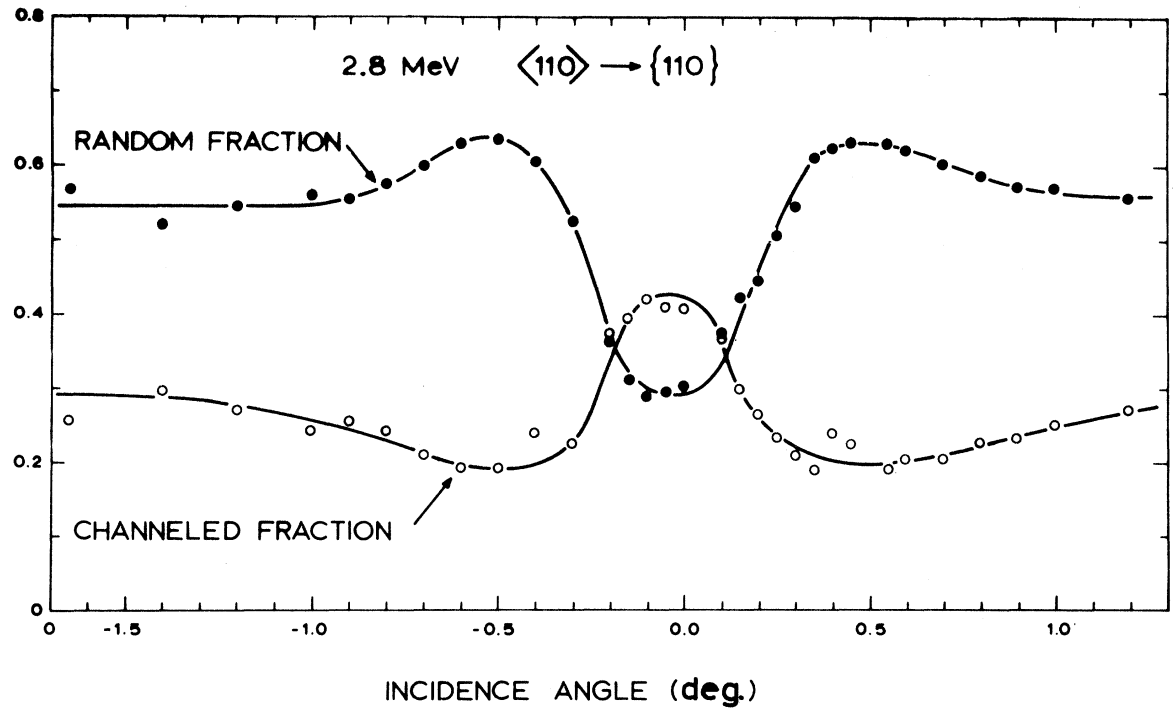

FIG. 8. Random and channeled fractions as a function of tilt angle from the ⟨110⟩ axis within the {110} plane. The beam energy is 2.8 MeV and the crystal thickness 5.6 μm. The meaning of these components is explained in the text.

neled with increasing depth in the crystal this maximum tends to level off, as already observed by Howe and Schmid.[6]

V. DISCUSSION

The interpretation of the experiments requires some care, because calculations indicate that usual concepts in terms of continuum theory can be misleading.

Our computer results as well as those of other authors[23] show that axially channeled particles wander from channel to channel: Only a very small fraction remains confined in the original channel (~1% of the total according to our calculations). The presence of these "hyperchanneled" particles has been recently observed by Appleton *et al.*[19] Since the ions overcome the interaxial barrier very easily already at zero degrees incidence, it seems very difficult to interpret the axial-planar transition in terms of a simple spatial potential barrier separating the two kinds of channeling.

On the other hand both calculations and experiments show that the transition from axial to planar regime is not a smooth one, but goes through a region of maximum stopping power and dechanneling. This is apparent also in the case of the transition from ⟨110⟩ axis to {111} plane and from ⟨111⟩ axis to {110} plane, which shows the difference between the axis and the most open plane passing through it (see Figs. 4, 6, and 7).

In order to explain these results, we report in Fig. 10 some typical ion paths, plotted by the computer and reduced to the initial channel, as done in Ref. 24, Fig. 10. All these paths refer to 2.8-MeV protons and a [011]→ (0$\bar{1}$1) transition.

Figure 10(a) shows an axial channeled path. The number of crossed channels is nine, but it is clearly seen that it avoids the strings; moreover

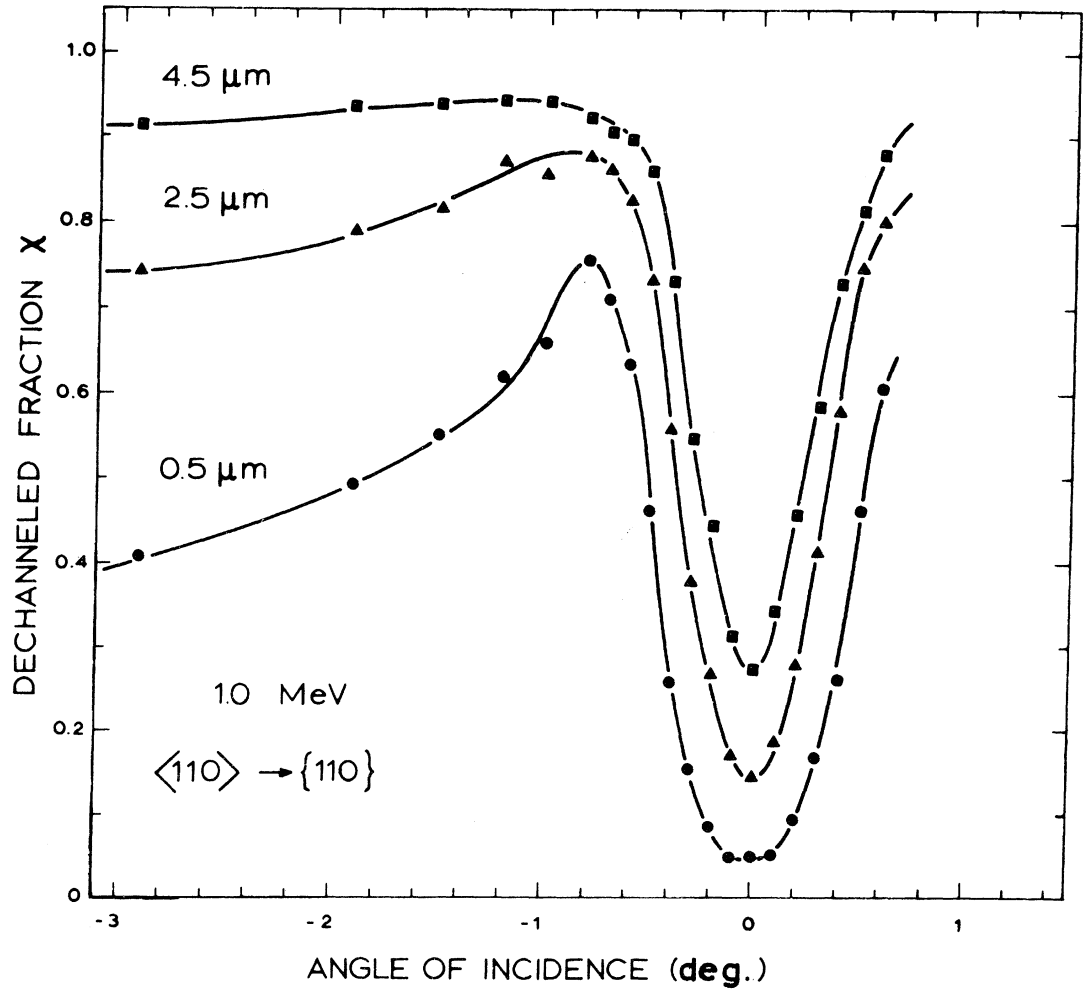

FIG. 9. Dechanneled fraction χ obtained by backscattering measurements vs tilt angle from the ⟨110⟩ axis within the {110} plane. The dechanneled fraction is measured at different depths into the crystal, as indicated. The beam energy is 1.0 MeV. The estimated error is not larger than the point size.

it can be seen that the particle goes out from the channel through the saddle points towards {111} planes. It appears that the channeled ion acquires a transverse energy of the order of 10 eV (as evaluated by the minimum distance of approach to the strings) corresponding to an angle of the order of 0.1°. This energy component is almost randomly distributed in the transverse plane: Therefore, we shall call it "radial" component.

When we tilt from the axis within a crystal plane, the ion acquires an additional transverse energy $E\theta^2$ parallel to the plane ("planar" component).

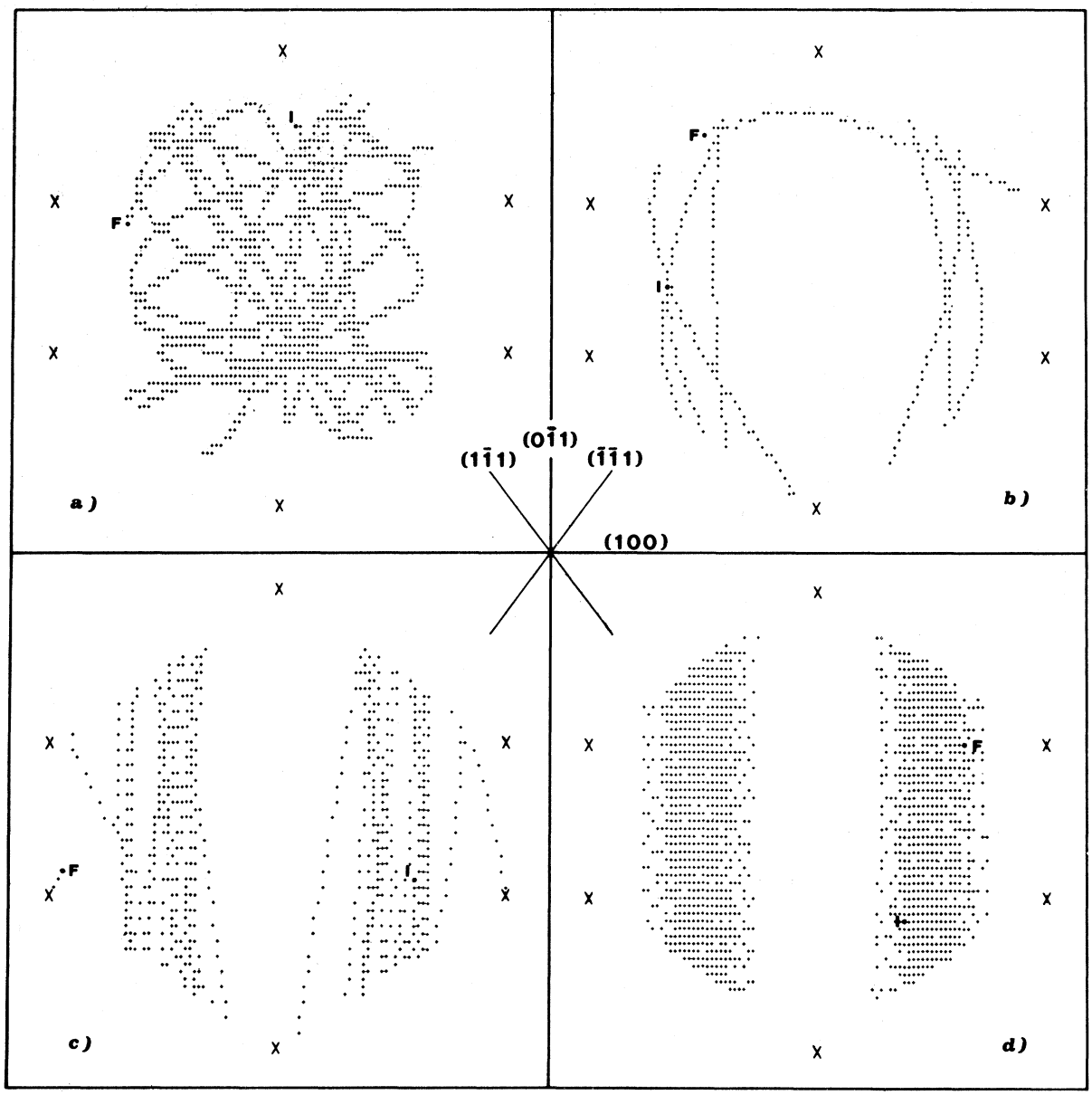

FIG. 10. Computed 2.8-MeV protons paths in a 5.6-μm-thick Si crystal for [011] → (0$\bar{1}$1) transition. The proton position is plotted every 20 Å and reduced to the initial channel. "I" and "F" indicate initial and final positions of the incident particle (when unspecified F lies at the end of the crystal) while "×" denotes the atomic rows. Crystal orientation is shown in the center. (a) [011] axial channeling. The number of channels crossed is nine. (b) 0.2° from the [011] axis within the (0$\bar{1}$1) plane. The part of the trajectory almost perpendicular to the (0$\bar{1}$1) plane and ending at *F* corresponds to the dechanneling of the particle. *F* lies at 0.62 μm. (c) 0.4° from the [011] axis within the (0$\bar{1}$1) plane. The final point *F*, at which the particle is just dechanneled, lies at 1.29 μm. (d) (0$\bar{1}$1) planar channeling (0.8° from the [011] axis). Notice that the appearance of a double strip is simply due to the reduction to the initial channel.

TABLE II. Measured values of the angle θ_t at which the stopping number $\bar{B}$ is maximum for various transitions and energies.

E (MeV)	⟨110⟩→{110}	⟨110⟩→{111}	⟨111⟩→{110}	⟨112⟩→{111}	⟨112⟩→{110}
1.0	0.80°	•••	0.40°	•••	•••
2.0	0.75°	0.20°	0.30°	0.15°	0.60°
2.8	0.40°	•••	•••	•••	•••

When the incidence angle is high enough so that the radial component is negligible compared to the planar one, we have the planar channeling shown in Fig. 10(d). In this case the radial component produces only oscillations between the planes and is not sufficient to bring the ion close to atoms. Incidentally it can be noted that in the case in which the ion starts in the central strip of the channel, i.e., inside an atomic plane, it is rapidly dechanneled, which is consistent with the well-known fact that surface dechanneling is higher for plane than for axis (see, e.g., p. 49 of Ref. 1).

In the intermediate angular region, the radial component is no longer negligible. This gives rise to a spreading out of the "planar" channeled paths in a direction perpendicular to crystal planes until the particle hits one atom. In the language of continuum theory it may be said that the angle with the strings is not high enough to smear out the atomic rows in the continuum plane. Therefore the particle can penetrate into the atomic planes because of the random transverse motion in the two-dimensional lattice of strings and is finally scattered away (see p. 25 of Ref. 1). Figures 10(b) and 10(c) clearly show this effect and explain both the great dechanneling and the maximum in the distribution of the stopping number $\bar{B}$ versus the tilt angle. In fact for the reason explained above also the few particles that remain channeled spend a part of their time in regions nearer to atoms than in purely axial or planar cases. Of course even these will be dechanneled with increasing crystal thickness.

Table II summarizes the angles θ_t at which $\bar{B}$ is maximum for various energies and transitions. Results are reported also for transitions not shown in the previous figures. For comparison Tables III shows Lindhard's critical angle ψ_1,[1] corrected for thermal vibrations according to Eq. (14) of Ref. 5.

In backscattering, the angular value of maximum yield when we move from axis to random is of the order of $\psi_1\sqrt{2}$ (see p. 16 of Ref. 1). Our observed values for the maximum $\bar{B}$ are of this order for the narrower planes {110} and much lower for the most open planes {111}. This result is consistent with the computed values of nuclear encounter probability reported by Barrett.[25]

In any case we would like to emphasize that care must be taken in comparing backscattering and transmission results, because in the former only particles with low impact parameters are recorded as dechanneled, while in the latter we include as dechanneled also particles sampling higher electron density without coming too close to atoms, so that these experiments can give different answers to the same question. Another possible reason of discrepancy between transmission and backscattering data, which goes in the opposite sense to the previous one, has been put forward by Altman *et al.*[22]: Nonchanneled particles also contribute to backscattering with trajectories which yield probabilities for scattering higher than particles with random paths.

Our computer results show on the other hand that ⟨110⟩ axial channeling contains also a planar channeled component along the most open planes {111} (ranging from 12.5% at 1-MeV proton energy and 2.45-μm crystal thickness to 8.5% at 2.8 MeV and 5.6 μm): Therefore, the interpretation of backscattering yields requires some care. In fact, both particles dechanneled from the axis and the most open planes at the same depth can contribute to the backscattering yield at a given energy. Since the experimental axial and planar dechanneling rates are different,[4] the ignorance of the amount of planar components makes ambiguous the interpretation of backscattered axial spectra in terms of purely axial channeling and misleading a comparison with theory. A systematic analysis by using both transmission technique with a collimated detector and backscattering technique can give information on the latter point.

Figure 11 compares the results of backscattering, transmission experiments and computations. Backscattering experiments and transmission computations give the dechanneled fraction as a function

TABLE III. Critical angle $\psi_{1/2}$ for axial channeling calculated by Eq. (14) of Ref. 5.

E (MeV)	$\psi_{1/2}$ (deg) ⟨110⟩	⟨111⟩	⟨112⟩
1.0	0.54	0.49	•••
2.0	0.38	0.35	0.29
2.8	0.32	•••	•••

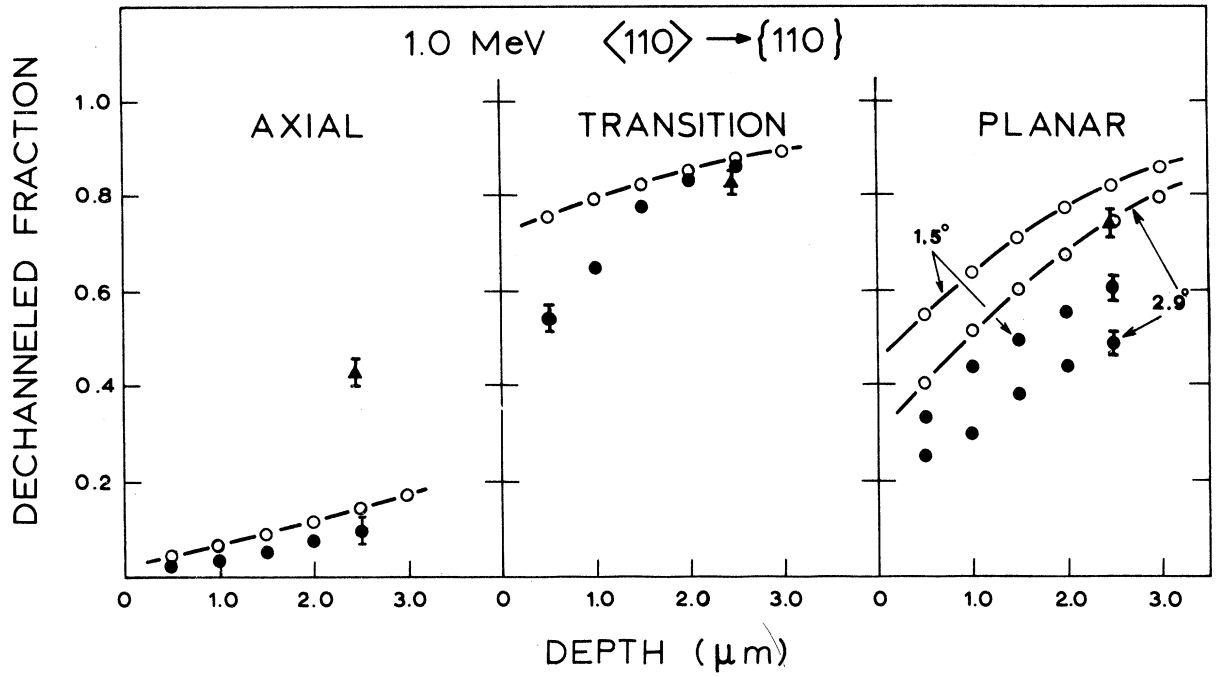

FIG. 11. Dechanneled fraction vs depth for 1.0-MeV protons in silicon. Tilt angles from the ⟨110⟩ axis within the {110} plane are reported in the figure for the planar case and is equal to 0.8° for the transition. Errors are reported only for some points. Open circles, backscattering experiments; filled triangles, transmission experiments; filled circles, transmission computations.

of depth, while transmission experiments give only the dechanneled fraction over the total thickness. With regard to the previously reported classification of the transmitted energy spectra components (see Sec. IV A) it must be pointed out that in this case the intermediate spectrum (c), probably because of energy resolution, turns out to be negligible.

Figure 11(a) shows that the dechanneled fraction obtained from backscattering is lower than the one obtained from transmission measurements in the axial case. This can be attributed to the above-mentioned fact that in the two types of experiments different ranges of impact parameters are involved to determine the dechanneled fraction.

From Fig. 11(c) we see on the contrary that in the planar case transmission and backscattering experiments are in agreement. On the other hand both figures show the already discussed underestimate of dechanneling in our calculations.

However, we believe that our statistical criterion for dechanneling can be of value for future developments of the computer model aiming at clarifying the differences between the two kinds of experiments.

The following conclusions can be drawn.

(i) According to calculations proper axial channeling is very rare and axially channeled particles wander from channel to channel. Moreover a non-negligible planar component along the most open planes is present.

(ii) Notwithstanding item (i), both experiments and calculations show a sharp distinction between axial and planar channeling; the transition being characterized by a maximum in stopping power of channeled particles and in the dechanneled fraction.

(iii) Computer simulations show that the transition is associated with some kind of instability of the planar trajectories, correlated with the relative values of transverse energy components.

(iv) Backscattering measurements confirm the general trend observed in transmission. The two kinds of experiments give complementary informations because they correspond to somewhat different physical situations; therefore, a direct comparison of the results requires some care.

ACKNOWLEDGMENTS

We wish to thank Professor I. Filosofo and the staff of Legnaro Laboratory for the technical assistance in the research, and F. Momo for the cooperation during the measurements.

APPENDIX

In backscattering experiments, the dechanneling rate is obtained by measuring the energy spectrum of backscattered particles, using both an aligned and a random primary beam. The comparison be-

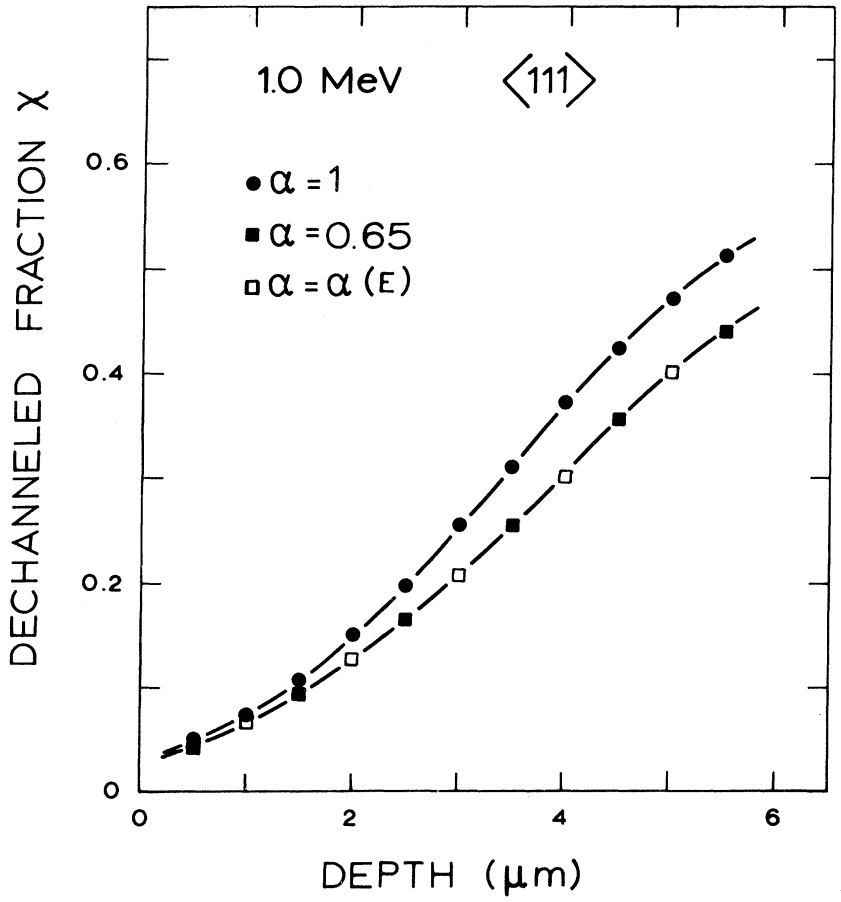

FIG. 12. Dechanneled fraction χ vs depth calculated from backscattering measurements. Beam energy, crystal orientation and used stopping power ratio α (see text) are reported in the figure.

tween aligned and random yield gives the beam dechanneled fraction as a function of the observed energy.

In order to convert energy to depth, the knowledge of the stopping power of channeled and random particles is needed. In several experimental works, the yield of aligned and random spectra were compared at the same energy, assuming the same stopping power for random and aligned particles. The use of a lower stopping power for channeled particles, not only gives different energy-depth scales for channeled and random particles, but also implies that channeled particles have an energy higher than that of the random ones at the same depth: Thus a correction factor must be introduced to account for the energy dependence of the cross section. Such a dependence can be directly derived from the random spectrum.

As an example we calculated the dechanneling rate of 1.0-MeV protons channeled along ⟨111⟩ axis in silicon, using for the ratio between the stopping power in channeling and random conditions,

$$\alpha = \left(\frac{dE}{dx}\right)_C \Big/ \left(\frac{dE}{dx}\right)_R$$

the values $\alpha = 1$ and $\alpha = 0.65$ and taking into account the energy dependence of α. The values $\alpha = 0.65$ and the energy dependence were obtained by our previous transmission experiments.[8]

The results are shown in Fig. 12. The value $\alpha = 1$ involves no corrections, thus the dechanneled fraction is the ratio between aligned and random yield at the same energy. It appears that the use of a lower stopping power for channeled particles decreases the dechanneling rate: It should be noted that this decrease is much more pronounced the lower is α, i.e., in more open channels.

In our case it makes no difference to neglect the dependence of α on energy, because in the energy range of the channeled path (1.0–0.8 MeV) α varies only from 0.65 to 0.67. However this correction could be important at higher depths in the crystal and at low values of E/A, A being the atomic mass of the projectile, because α varies more rapidly with decreasing E/A.[8,13]

We observe that with the transmission technique we measure the most probable value of the stopping power for the best channeled particles. On the other hand backscattered particles could suffer higher energy losses, especially at the end of the path, before the scattering, where the electron density is higher. As a consequence the true α

value for backscattered particles will lie somewhat between the channeled and random value (see also the discussion at p. 138 of Ref. 26). However an indirect measurement of α using low-impact-parameter processes [i.e., wide-angle Rutherford scattering and the resonant ^{28}Si (p, γ) ^{29}P reaction] gave $\alpha = 0.58 \pm 0.04$ for 1.6-MeV protons channeled along the $\langle 111 \rangle$ axis in silicon,[27] in excellent agreement with the value obtained by transmission[8] $\alpha = (0.61 \pm 0.03)$. Therefore, in our dechanneling calculations we always assumed the α values obtained by transmission experiments.

---

*The experimental part was performed at Laboratori Nazionali Legnaro, Italy. Research supported in part by G.N.S.M. and in part by La.M.El. Laboratory of C.N.R.

†Istituto Chimico, Facoltà di Ingegneria, Università di Bologna, Bologna, Italy.

[1]J. Lindhard, K. Dan. Vidensk. Selsk. Mat.-Fys. Medd. **34**, 14 (1965).

[2]B. R. Appleton, C. Erginsoy, and W. M. Gibson, Phys. Rev. **161**, 330 (1967).

[3]J. U. Andersen, J. A. Davies, K. O. Nielsen, and S. L. Andersen, Nucl. Instrum. Methods **38**, 210 (1965).

[4]J. A. Davies, J. Denhartog, and J. L. Whitton, Phys. Rev. **165**, 345 (1968).

[5]J. H. Barrett, Phys. Rev. B **3**, 1527 (1971).

[6]L. M. Howe and S. Schmid, Can. J. Phys. **49**, 2321 (1971).

[7]G. Dearnaley, B. W. Farmery, I. V. Mitchell, R. S. Nelson, and M. W. Thompson, in Proceedings of the International Conference Solid State Research with Accelerators, Brookhaven 1967, edited by A. N. Goland, BNL Report No. 50083, p. 125 (unpublished); G. Dearnaley, I. V. Mitchell, R. S. Nelson, B. W. Farmery, and M. W. Thompson, Philos. Mag. **18**, 985 (1968).

[8]G. Della Mea, A. V. Drigo, S. Lo Russo, P. Mazzoldi, and G. G. Bentini, Phys. Rev. Lett. **27**, 1194 (1971); Radiat. Eff. **13**, 115 (1972).

[9]R. L. Meek, J. Electrochem. Soc. **118**, 1240 (1971).

[10]C. F. Williamson, J. F. Boujot, and J. Picard, Rapport CEA, Report No. R-3042 (1966) (unpublished).

[11]A. Desalvo, R. Rosa and F. Zignani, Nuovo Cimento Lett. **2**, 390 (1971); J. Appl. Phys. **43**, 3755 (1972).

[12]C. Varelas and J. Biersack, Nucl. Instrum. Methods **79**, 213 (1970).

[13]F. H. Eisen, G. J. Clark, J. Bøttiger, and J. M. Poate, Radiat. Eff. **13**, 93 (1972).

[14]J. Lindhard and M. Scharff, K. Dan. Vidensk. Selsk. Mat.-Fys. Medd. 27, 15 (1953).

[15]F. H. Eisen and M. T. Robinson, Phys. Rev. B **4**, 1457 (1971); M. T. Robinson, Phys. Rev. B **4**, 1461 (1971).

[16]Y. H. Ohtsuki, M. Mizuno, and M. Kitagawa, J. Phys. Soc. Jap. **31**, 1109 (1971); M. Kitagawa and Y. H. Ohtsuki, Phys. Rev. B **4**, 3418 (1972).

[17]J. Lindhard, K. Dan. Vidensk. Selsk. Mat.-Fys. Medd. 28, 8 (1954). Since we do not assume any equipartition, we preferred to use Eq. (4) instead of Eq. (4.3) of Ref. 1. This implies that at midchannel axis, where energy loss is due to valence electrons (see Ref. 2), we take into account close collisions with the latter.

[18]K. Björkqvist, B. Cartling, and B. Domeij, Radiat. Eff. **12**, 267 (1972).

[19]B. R. Appleton, J. H. Barrett, T. S. Noggle, and C. D. Moak, Radiat. Eff. **13**, 171 (1972); B. R. Appleton, C. D. Moak, T. S. Noggle, and J. H. Barrett, Phys. Rev. Lett. **28**, 1307 (1972).

[20]A. R. Sattler and G. Dearnaley, Phys. Rev. **161**, 244 (1967).

[21]B. R. Appleton, L. C. Feldman, and W. L. Brown, Proceedings of the International Conference on Solid State Research with Accelerators, Brookhaven, 1967, edited by A. N. Goland, BNL Report No. 50083, p. 45 (unpublished).

[22]M. R. Altman, L. C. Feldman, and W. M. Gibson, Phys. Rev. Lett. **24**, 464 (1970).

[23]M. T. Robinson and O. S. Oen, Phys. Rev. **132**, 2385 (1963).

[24]S. Datz, C. Erginsoy, G. Leibfried, and H. O. Lutz, Annu. Rev. Nucl. Sci. **17**, 129 (1967).

[25]J. H. Barrett, Phys. Rev. **166**, 219 (1968); T. S. Noggle and J. H. Barrett, Phys. Status Solidi **36**, 761 (1969).

[26]J. W. Mayer, L. Eriksson, and J. A. Davies, *Ion Implantation in Semiconductors* (Academic, New York, 1970).

[27]G. Della Mea, A. V. Drigo, S. Lo Russo, and P. Mazzoldi, Atti Acc. Naz. Lincei L11, 727 (1972).